JOURNAL OF CATALYSIS 92, 364–375 (1985)

A Single Crystal Study of the Silver-Catalysed Selective Oxidation and Total Oxidation of Ethylene

ROBERT B. GRANT AND RICHARD M. LAMBERT[1]

Department of Physical Chemistry, University of Cambridge, Cambridge CB2 1EP, England

Received May 3, 1984; revised July 26, 1984

Ethylene oxidation has been investigated on a well-characterised Ag(111) single crystal surface at pressures of up to 50 Torr. In the absence of promoters and moderators, chemisorbed atomic oxygen reacts with *adsorbed* ethylene to yield both ethylene oxide and (CO_2 + H_2O). Chemisorbed dioxygen, though present, appears to play no direct role in either of these reactions; the presence of subsurface oxygen is necessary for selective oxidation but not for total oxidation. Batch reactor studies yield rate parameters for both partial and total oxidation which are consistent with the values reported for conventional supported catalysts; selectivity decreases with increasing temperature, pressure, and ethylene coverage. Acetaldehyde, acetic acid, and oxalic acid are identified as reaction intermediates in the pathway to CO_2 formation. Results for the oxidation of C_2D_4 confirm these observations, and the observed kinetic isotope effect indicates that H-transfer rather than C–C cleavage is rate-determining in the combustion of both ethylene and ethylene oxide. Possible reaction pathways and mechanisms are examined.

INTRODUCTION

Silver is a uniquely effective catalyst for the selective oxidation of ethylene to ethylene oxide, and this reaction has been the subject of many mechanist studies, the majority of which have been carried out on conventional supported Ag catalysts or on Ag powders. The subject has been extensively reviewed (*1–4*) and it is generally accepted that the observed overall behaviour can be understood in terms of the following scheme

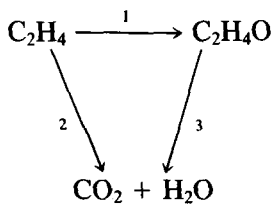

However, the detailed mechanisms of Reactions 1–3 are still very much a matter for debate. Much of the thinking in this field has been guided by the mechanism proposed by Kilty and Sachtler (*1*) on the basis of their ir studies on supported Ag. These authors suggested that adsorbed *dioxygen* [O_2(a)] is the crucial surface species which leads to epoxide formation; CO_2 + H_2O production was ascribed to chemisorbed *atomic* oxygen [O(a)]. Variations on this basic idea have also been proposed (*5*). An alternative hypothesis, also derived from ir measurements on supported Ag, proposes that O(a) leads to *both* epoxidation and complete oxidation (*6, 7*). Cant and Hall (*8*) used the deuterium kinetic isotope effect to arrive at yet a third mechanism, namely that O_2(a) is the common precursor for both ethylene oxide and (CO_2 + H_2O). This is also the conclusion favoured by Akimoto and co-workers (*9*). So-called surface science techniques have been used to characterise molecularly and dissociatively adsorbed oxygen on a variety of Ag surfaces (*10–15*) though the reactions of these species with ethylene were not investigated. Experiments using N_2O as the oxidant rather than O_2 have been carried out to test the various hypotheses (*16–18*) but the

[1] To whom correspondence should be addressed.

0021-9517/85 $3.00

results have been somewhat equivocal (*19, 20*). Yet other work has pointed to the likely relevance of *dissolved* oxygen [O(d)] to the selective oxidation reaction (*21–23*). A few studies of C_2H_4/O_2 reactivity on macroscopic single crystal or polycrystalline Ag specimens have been performed (*24–29*): in every case the authors were able to observe only the total oxidation reaction. Failure to detect partial oxidation may in part have been the result of working with very small sample areas at low pressures.

The present paper reports on the first every investigation of the mechanisms of selective oxidation and total oxidation of ethylene using a well-characterised Ag single crystal surface. The (111) plane was chosen because it is likely to be the most important crystal face in a real catalyst; it is in fact the most difficult face to work with because it exhibits a very small sticking probability for oxygen ($\sim 10^{-6}$) even when atomically clean. Auger electron spectroscopy was used to characterise and monitor the condition of the crystal surface, while reactive studies could be made in either of two modes. Temperature-programmed reaction (TPR) measurements under ultrahigh vacuum were used to examine the reaction between surface species previously adsorbed at much higher pressures; alternatively, the crystal was operated isothermally as a catalyst in batch reactor mode at a total pressure of up to 50 Torr. Some experiments with C_2D_6 were carried out in order to elucidate certain aspects of the mechanism, and reaction intermediates in the further oxidation of ethylene oxide have been identified.

METHODS

The apparatus consisted of an ultrahigh vacuum (UHV) chamber coupled directly to a high-pressure reactor cell. The UHV chamber was equipped with the usual facilities for LEED/Auger analysis and Ar^+ etching. It also contained a computer-controlled quadrupole mass spectrometer which could *simultaneously* record TPR spectra from up to eight different ion signals. This greatly increases the reliability of the experimental data. The specimen could be rapidly transferred between the UHV chamber and a 75-ml reactor *via* a special gate valve; reactant and product partial pressures and their time dependence were monitored by a second quadrupole mass spectrometer sampling through a variable leak valve. Transfer time in the reverse direction from ~ 10 to 10^{-9} Torr was typically 1 min. The orientation, cutting and polishing of the Ag(111) specimen followed standard methods, and research grade O_2 and C_2H_4 were used throughout the work; the C_2D_4 was 95% (MSD Ltd).

RESULTS

Multimass Temperature-Programmed Reaction

In agreement with earlier work (*30, 31*) it was found that no ethylene adsorption detectable either by Auger spectroscopy or by thermal desorption measurements occurred on clean, annealed Ag(111) at 300 K. Ethylene pressures as high as 100 Torr were employed. However, at 300 K ethylene does slowly chemisorb on a surface presaturated with oxygen at 300 K. The oxygen dosing was carried out at 0.1 Torr and was equivalent to an exposure of $\sim 5 \times 10^6$ L (1L = 10^{-6} Torr s). This procedure produces an oxygen fractional surface coverage of $\theta \geq 0.1$ consisting mainly of chemisorbed atomic oxygen [O(a)] and ~15% *chemisorbed* dioxygen (*32*). Identification of the 380 and 580 K oxygen thermal desorption peaks with O_2(a) and O(a), respectively, is consistent with their oxygen isotope scrambling characteristics; the estimated lower bound on the surface coverage is based on LEED observations and is in agreement with independent ellipsometric studies on the Ag(111)–O_2 system (see Ref. (*32*) and references therein). After withdrawing the specimen from the reactor cell simultaneous TPR spectra were recorded at 44, 32, 28, and 18 a.m.u. with a heating rate of 13 K

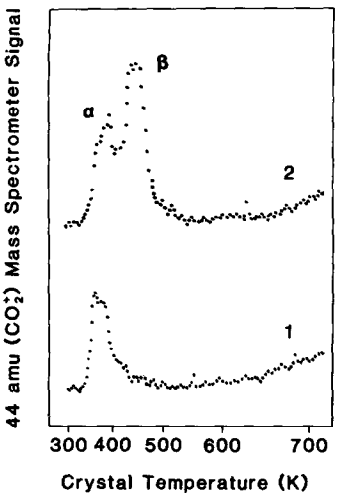

FIG. 1. CO_2 TPR spectra for C_2H_4 oxidation. (1) On clean Ag(111). (2) In the presence of O(d). Dose was 5 × 10^6 L O_2 followed by 9 × 10^6 L C_2H_4. Heating rate 13 K s^{-1}.

s^{-1}. A typical CO_2 spectrum obtained at 44 a.m.u. under these conditions is shown in Fig. 1 (spectrum 1); it consists of a single peak (α) at 380 K. The identification of this with CO_2 was confirmed by simultaneously recording the 28-a.m.u. spectrum (CO^+). This mirrors the 44-a.m.u. spectrum and the CO_2^+/CO^+ relative intensity agrees with that measured for gaseous CO_2 in a separate control experiment. H_2O is also evolved in such TPR experiments (peak temperature < 340 K) but no ethylene oxide was detectable. The H_2O spectra were somewhat irreproducible due to adsorption/desorption effects at the vessel walls; they were not therefore routinely monitored. The O_2 spectra (32 a.m.u.) indicated that adsorbed ethylene reacted only with O(a), attenuating the ~580 K O_2 peak (*32*); the ~380 K dioxygen peak was unaffected by the reaction.

It was however found that the clean surface could be *activated* towards selective oxidation by annealing the specimen at 425 K in a 6:1 mixture of oxygen and ethylene at 10 Torr for about 1 h. Auger spectroscopy showed that this treatment led to a build-up of O(d) in the subsurface region but no detectable accumulation of Cl, C, or any other impurities. Reaction of chemisorbed ethylene and oxygen on this surface (henceforth referred to as the active surface) produced a new feature (β) in the CO_2 TPR spectrum with a peak temperature of ~450 K (see Fig. 1, spectrum 2); this was accompanied by an associated H_2O peak at the same temperature. A weak 29-a.m.u. (CHO^+) signal giving a peak at ~360 K was also produced. Multimass TPR experiments were carried out to examine signals which correlated with the 29-a.m.u. signal. None were detected at 46, 31, or 30 a.m.u., but coincident TPR peaks *were* found at 43, 42, and 15 a.m.u. This suggests that the TPR peak at ~360 K is associated with ethylene oxide and/or acetaldehyde. Reference mass spectrometer fragmentation patterns for gaseous CH_3CHO and C_2H_4O were measured in the apparatus and a detailed quantitative comparison made with the 43, 42, 29, and 15-a.m.u. TPR spectra. The results indicate that the ~360 K TPR peak is due to the desorption of a mixture of ethylene oxide (35 ± 15%) with acetaldehyde. (Control experiments on the reaction of CO with adsorbed oxygen confirmed that the 29-a.m.u. signal was not due to $^{13}CO_2$ resulting from the oxidation of adventitiously adsorbed background impurities (e.g., CO or C_2H_2).)

The role of both types of oxygen species in selective oxidation was investigated by TPR measurements in the following four ways:

1. The ethylene oxide yield at 29 a.m.u. from a surface bearing both O(a) *and* O_2(a) was compared with that from surface bearing O(a) alone, O_2(a) being removed by heating to ~475 K prior to ethylene dosing. Typical results of multimass TPR sweeps are illustrated in Figs. 2a and b. It can be seen that prior removal of dioxygen has no discernible effect on the yield of ethylene oxide.

2. The results for oxygen predosing at ~1 Torr were compared with those obtained for the *same oxygen exposure* at

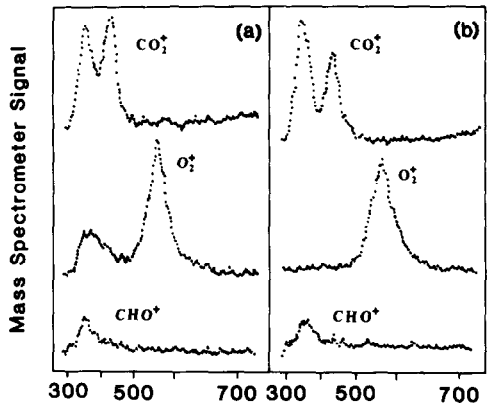

FIG. 2. Multimass TPR spectra for C_2H_4 oxidation on active Ag(111). (a) In the presence of dioxygen. (b) Without dioxygen. Other conditions as for Fig. 1.

$\sim 10^{-2}$ Torr. The latter procedure leads to no uptake of O_2(a) while leaving the O(a) uptake essentially unchanged (*32*). Again, the yield of ethylene oxide was the same in the two types of experiment.

3. The O_2(a) yield from (say) an oxygen-saturated surface was independent of whether or not ethylene adsorption and a subsequent temperature-programmed reaction were carried out. On the other hand, the O(a) population was very substantially attenuated by reaction.

4. The dependence of the ethylene oxide yield on the coverage of both types of oxygen species was investigated systematically. It was found to be independent of dioxygen coverage but approximately proportional to O(a) coverage in the range $0.03 < \theta < 0.09$. ($\theta \sim 0.1$ corresponds to the saturation uptake of O(a) on clean Ag(111) at 300 K (*32*)).

Thus the evidence indicates that O_2(a) plays no direct role in either the partial oxidation or in the total oxidation of ethylene under these conditions; O(a) is directly involved in both reactions.

The total oxidation reaction was investigated quantitatively by following CO_2 production at 44 a.m.u. Figure 3 shows the CO_2 yield from an oxygen presaturated surface as a function of subsequent ethylene dose. At very low ethylene exposures ($\sim 2 \times 10^6$ L) only the β-CO_2 feature is present; increased ethylene exposure leads to the appearance of the α-CO_2 feature whose intensity eventually becomes approximately equal to that of β-CO_2. The total CO_2 yield increases to a maximum at an ethylene exposure of $\sim 7.5 \times 10^7$ L (Fig. 4a) after which there is a gradual decrease. At very high ethylene exposures ($>10^8$ L) Auger spectroscopy showed that residual carbon was present at the end of the TPR scan; this material could also be detected by oxygen titration in a subsequent experiment: C(a) + 2O(a) $\rightarrow$ CO_2(g).

In these experiments unreacted O(a) undergoes recombination and eventual desorption as manifested by the ~ 580 K O_2 peak. The variation of this residual O(a) concentration with ethylene dosage is shown in Fig. 4b; comparison with the data in Fig. 4a shows that CO_2 production continues to increase with ethylene coverage even after all the surface atomic oxygen has reacted. In fact, quantitative measurements indicated that the total TPR yield of oxy-

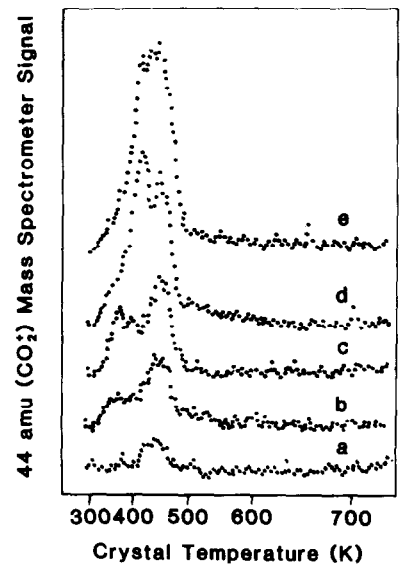

FIG. 3. CO_2 TPR spectra for C_2H_4 oxidation on active Ag(111) as a function of ethylene coverage. (a)–(e) correspond to ethylene doses of 2, 6, 9, 30, $\times 10^6$ L respectively. Other conditions as for Fig. 1.

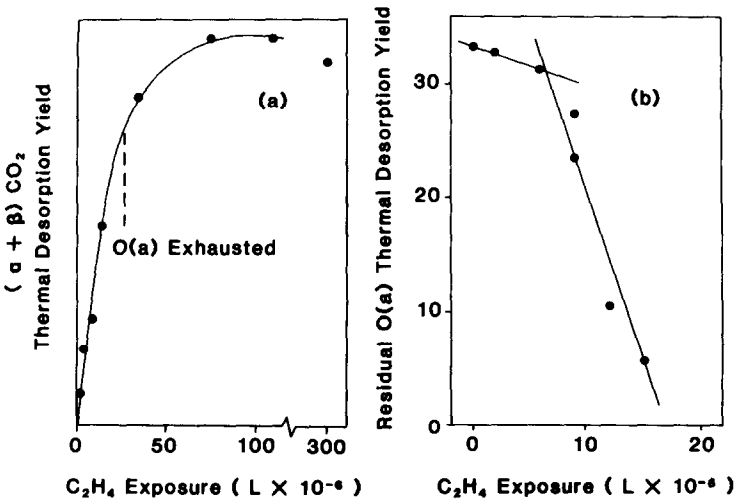

FIG. 4. (a) CO_2 TPR yield as a function of ethylene exposure for the oxygen-saturated surface. (b) Unreacted O(a) as a function of C_2H_4 exposure for an initially oxygen-saturated surface.

gen-containing species (C_2H_4O, CO_2, H_2O, CO_2) normally exceeds that expected from the initially chemisorbed oxygen by ~30%.

The nature of the α- and β-CO_2 peaks was examined further by studying the CO_2 TPR spectra resulting from the coadsorption and reaction of oxygen with *ethylene oxide* itself (Fig. 5). It can be seen that this reaction leads to only the β-CO_2 peak; the small shoulder which lies to lower temperature is due to the parent ion signal from desorbing unreacted ethylene oxide (cf. with the 29-a.m.u. signal (CHO^+) from ethylene oxide which is also shown in Fig. 5). This strongly suggests that the β-CO_2 peak which is observed when *ethylene* is the reactant may be ascribed to the further oxidation of newly formed ethylene oxide. In these experiments the yield of unreacted O(a) fell linearly with ethylene oxide exposure giving a gradient of -6.0×10^6 atoms L^{-1} cm^{-2} (Fig. 6) indicating a constant net probability for adsorption and reaction at these oxygen coverages ($\theta \leq 0.09$).

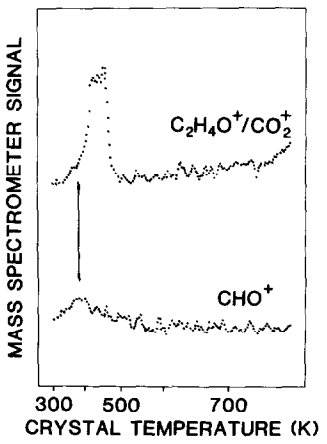

FIG. 5. Multimass TPR spectra for *ethylene oxide* oxidation on active Ag(111). 5×10^6 L O_2 followed by 1.2×10^7 L C_2H_4O at 300 K.

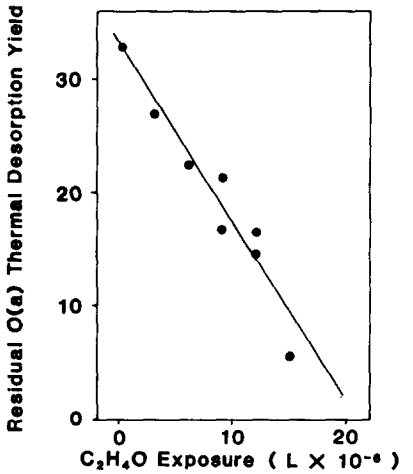

FIG. 6. C_2H_4O oxidation by TPR. Unreacted O(a) as a function of *ethylene oxide* exposure.

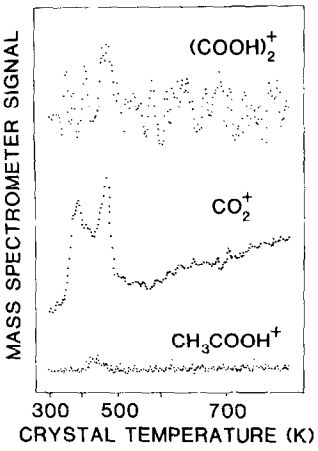

FIG. 7. Ethylene oxidation TPR spectra showing reaction intermediates. 5×10^6 L O_2 followed by 9×10^6 L ethylene.

During the TP reaction of ethylene with oxygen, weak signals were detected at 60 and 55 a.m.u. possibly corresponding to the production of CH_3COOH and $(COOH)_2$, respectively (Fig. 7). The former feature precedes the β-CO_2 peak whereas the latter (very weak) feature is almost coincident with the β-CO_2 peak, suggesting that acetic and oxalic acids may be sequential intermediates in the further oxidation of ethylene oxide. This behaviour was investigated further using C_2D_4 in place of C_2H_4; qualitatively, the two sets of results were similar, but there were some notable differences:

1. The 48- and 30-a.m.u. spectra ($C_2D_4O^+$, CDO^+) display a pronounced additional feature which correlates with the β-CO_2 peak (Fig. 8A). Signals at these masses could only be due to C_2D_4O and CD_3CHO, both of which would also yield a signal at 46 a.m.u. ($C_2D_3O^+$); this too is evident in Fig. 8A. With this clue from the C_2D_4 experiments, careful examination at high gain of the 29-a.m.u. (CHO^+) spectra from C_2H_4 oxidation revealed the presence of a similar (weak) peak which correlates with β-CO_2.

2. There are very strong features in the $C_2D_3O^+$ spectrum which are not present in the corresponding $C_2H_3O^+$ spectrum.

3. The yield of CD_3COOD is ~7 times greater than that of CH_3COOH (Fig. 8B). The intense feature in the 46-a.m.u. spectrum is due to the ions $COOD^+$ and CD_3CO^+; these are the principal fragment ions of CD_3COOD.

In making these comparisons between the two cases it is assumed that the molecular ionisation cross sections and fragmentation patterns are not drastically changed by D for H substitution. The available data (*33*, *34*) suggest that both assumptions are valid. The experiments with deuteroethylene therefore show that the yields of C_2D_4O/CD_3CDO and of CD_3COOD are ~55 and ~770% greater than those of their hydrogen analogues. They also permit us to confirm that C_2D_4O/CD_3CDO are produced in these experiments because observation of the parent molecular ions (48 a.m.u.) is no longer interfered with by CO_2 (44 a.m.u.). In summary, the multimass TPR data show that: (a) C_2H_4O is produced by reaction of C_2H_4 with O(a) in the presence of O(d). (b) The β-CO_2 feature is due to further oxidation of ethylene oxide. (c) Intermediates in this further oxidation pathway are detectable (CH_3CHO, CH_3COOH, $(COOH)_2$). (d) There are pronounced kinetic isotope effects.

Batch Reactor Studies at Elevated Pressure

The kinetics of the partial and total oxidation reactions were examined by measuring the rate of product formation in the pressure cell. C_2H_4O was monitored by means of the 42-a.m.u. fragment ion ($C_2H_2O^+$); although this is the least intense fragment ion from ethylene oxide, it is completely free from mass interference due to other species. Total oxidation was followed by means of the CO_2^+ signal at 44 a.m.u.; since the selective oxidation rate was about one-tenth of the total oxidation rate, the small contribution at 44 a.m.u. due to $C_2H_4O^+$ caused no significant difficulty. A 1:1 reaction mixture was used throughout the work, thus avoiding the buildup of surface carbon which occurs in ethylene-rich

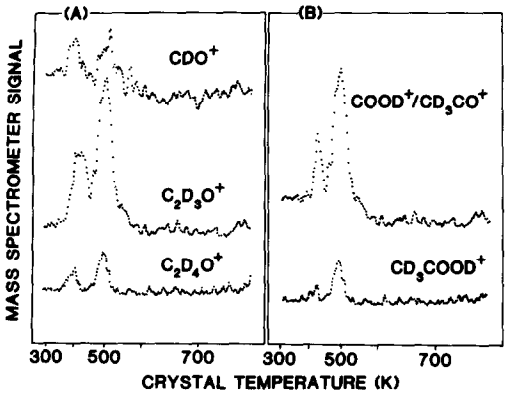

FIG. 8. Deuteroethylene oxidation. (A) Showing detection of ethylene oxide as parent ion *and* desorption of intermediates. (B) Desorption of reaction intermediates.

systems (*25*); the conversion level was ≤10%. Control experiments were performed on the Ta specimen support wires alone (~0.6 cm^2) with the crystal removed from the system. These showed that the rate of ethylene oxide production by the supports was undetectably small (<8.0 × 10^{12} molecule cm^{-2} s^{-1}); the rate of CO_2 production was <1% of that with the Ag(111) specimen present.

An Arrhenius plot for CO_2 production at a total pressure of 10 Torr is shown in Fig. 9a; this yields an activation energy (E_a) of 50 ± 1 kJ mol^{-1} and preexponential factor of ~4.5 × 10^{20} s^{-1}. A similar plot for the selective oxidation reaction gives E_a = 45 ± 4 kJ mol^{-1} and a preexponential factor of ~5.5 × 10^{18} s^{-1} (Fig. 9b). The pressure dependence of the rate parameters for both reactions is summarised in Tables 1 and 2. It can be seen that the selectivity falls from ~23 to ~9% as the pressure is increased from 5 to 50 Torr. Figure 10 shows the temperature dependence of the activity and the selectivity of active Ag(111) towards ordinary C_2H_4. At 500 K and 10 Torr the activity (½ rate of CO_2 formation + rate of C_2H_4O formation) is 4.2 × 10^{14} molecules cm^{-2} s^{-1} and the selectivity [defined as (C_2H_4O rate)/

TABLE 1

Rate Parameters of CO_2 Production (T.O.N. = Turnover Number)

Pressure (Torr)	R_{CO_2}[a] (molecules s^{-1} cm^{-2})	T.O.N.[a] (molecules $site^{-1}$ s^{-1})	E_a (kJ mol^{-1})
5	2.9 × 10^{14}	0.20	52 ± 3
10	7.2 × 10^{14}	0.50	50 ± 1
50	3.2 × 10^{15}	2.23	61 ± 4

[a] Turnover number. 500 K, 1 : 1 mixture C_2H_4 : O_2.

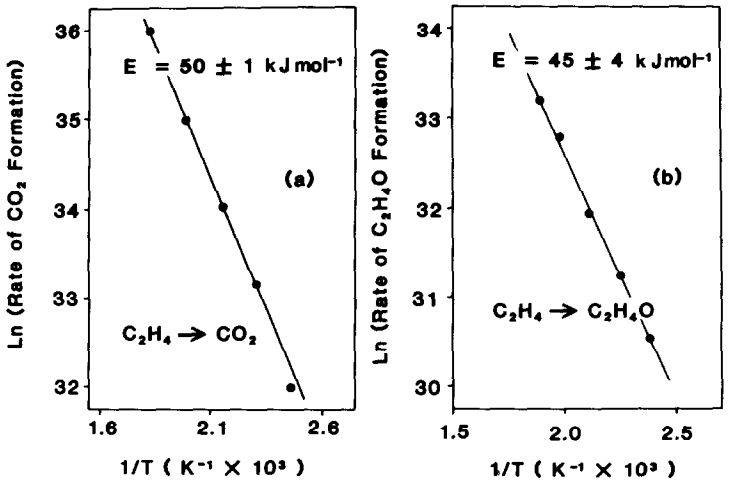

FIG. 9. Arrhenius plots for ethylene oxidation on Ag(111) in batch mode. 1 : 1 mixture of C_2H_4 and O_2 at 10 Torr. (a) Total oxidation and (b) selective oxidation.

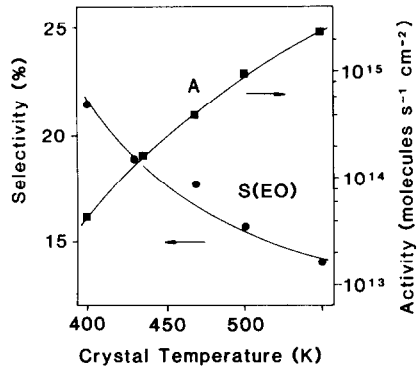

FIG. 10. Temperature dependence of activity (A) and selectivity S(EO). In terms of rates (R) these are given by $S(EO) = R(EO)/-R(E)$; $A = R(EO) + (\frac{1}{2})R(CO_2) = -R(E)$. Conditions as for Fig. 9.

(C_2H_4O rate + CO_2 rate)] is ~14%. Replacing C_2H_4 by C_2D_4 results in very similar activity (e.g., 5.7×10^{14} molecules cm^{-2} s^{-1} at 500 K) but the selectivity is increased to ~70%. Table 3 sets out the apparent kinetic isotope effects (k_D/k_H) for the total oxidation and partial oxidation reactions at 500 K. Similar behaviour has been reported for oxidised Ag sponge (*8*) and Ag powder catalysts (*45*); the present observation appears to be the first of its kind on a single crystal surface.

DISCUSSION

The first point to establish is that the chemistry being examined here really is relevant to that which occurs on practical high area catalysts in conventional studies. That this *is* in fact the case is strongly suggested by the results gathered in Table 4 which refer to measurements made at 10 Torr. The single crystal activation energies for C_2H_4O formation, CO_2 formation, and the specific rate for CO_2 production all lie within the range of reported values obtained from more traditional studies. As already noted, this is the first observation of selective oxidation over a single crystal. Other authors have however attempted to investigate the *total* oxidation reaction over single crystal Ag at low pressures. These studies gave low or very low values for the activation energy to CO_2 formation (*25, 27*);

TABLE 2

Rate Parameters of Ethylene Oxide (EO) Production

Pressure (Torr)	$R^a_{C_2H_4O}$ (molecules s^{-1} cm^{-2})	T.O.N.[a] (molecules site^{-1} s^{-1})	E_a (kJ mol^{-1})	S(EO) (%)
5	4.4×10^{13}	0.03	47 ± 8	23
10	6.1×10^{13}	0.04	45 ± 4	14
10[b]	1.1×10^{14}	0.07	51 ± 5	23
50	1.5×10^{14}	0.10	43 ± 2	9

[a] 500 K, 1:1 mixture C_2H_4:O_2.
[b] Monitoring 43 a.m.u.

TABLE 3

Kinetic Isotope Effects in Total and Partial Oxidation

	Rate of formation (molecules s^{-1} cm^{-2})[a]	
	CO_2	C_2H_4O
C_2H_4	7.2×10^{14}	6.1×10^{13}
C_2D_4[b]	3.4×10^{14}	4.0×10^{14}
k_D/k_H	0.5	6.5

[a] 500 K, 1:1 mixture C_2H_4O:O_2 at 10 Torr.
[b] After taking account of the relative sensitivities, C_2H_4O:C_2D_4O.

TABLE 4

Comparison of Rate Parameters on Single Crystal and Conventional Silver Catalysts

$E_a(C_2H_4O)$ (kJ mol^{-1})	$E_a(CO_2)$ (kJ mol^{-1})	R_{CO_2} (T = 500 K) (molecules s^{-1} cm^{-2})	Reference
45.0	50.0	7.2×10^{14}	This work (single crystal)
58.8	72.2	—	*9*
48.7	63.4	1.0×10^{14}	*41*
72.2	57.1	3.5×10^{14}	*41*
47.0	60.9	—	*42*
—	42.0	—	*43*
90.0	122.0	—	*44*
—	96.6	5.6×10^{14}	*29*
—	96.2	1.1×10^{15}	*28*

they also gave reaction probabilities which were unusually high ($\sim 10^{-3}$) compared to the values commonly encountered ($\sim 10^{-8}$) on supported catalysts (*28*). A likely explanation for this (*24*) is that small quantities of acetylene were present in the low-pressure single crystal studies. The reaction probability of acetylene with O(a) is close to unity (*24, 26, 35*); trace impurities could therefore have a profound effect. It seems possible that the source of this acetylene was a dehydrogenation reaction taking place at the stainless-steel walls of the gas-handling apparatus (*24*); a glass manifold was used in the present work. Our TPR results (Fig. 4b) suggest a combined adsorption and reaction probability of $\sim 10^{-9}$ at 300 K, while extrapolation of the batch reactor results to 300 K predicts a reaction probability for CO_2 formation of $\sim 5 \times 10^{-10}$. These figures are in satisfactory agreement with each other and with published data for conventional catalysts. The abrupt change in slope which is evident in Fig. 4b cannot be associated with the decrease in selectivity which undoubtedly *does* occur with increasing ethylene coverage, because under the conditions of the TPR experiments most of the ethylene oxide is further oxidised to $CO_2 + H_2O$. It must therefore imply that for ethylene (unlike ethylene oxide, see Fig. 6) the sticking probability changes with coverage.

Dissolved oxygen renders the surface active towards selective oxidation (Fig. 2) while also increasing the activity for CO_2 formation (Fig. 1). It is evident that the latter effect is associated with the further oxidation of ethylene oxide (β-CO_2, Figs. 1 and 5). The results in Fig. 4b indicate that this O(d) can participate *directly* in CO_2 production (though not in C_2H_4O formation) because the CO_2 yield continues to rise with ethylene exposure beyond the stage at which all the O(a) is consumed.

We may begin by suggesting an overall scheme in which stoichiometric balancing has been neglected in the interests of simplicity of presentation.

Primary stage

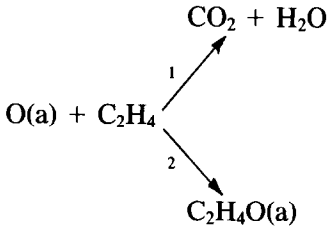

For the moment, we do not specify the exact state of the ethylene molecule.

Secondary stage

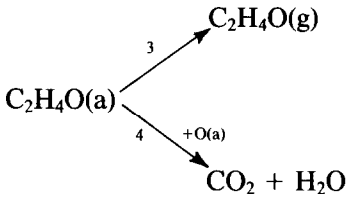

The overall selectivity is then determined by the product of the branching ratios for the primary and secondary steps. For the purposes of discussion, it is convenient to consider next the details of the secondary chemistry. Reaction 4 gives the β-CO_2 peak, and the observation of carboxylic acid intermediates suggests that it follows the sequence

$$C_2H_4O \xrightarrow{4a} CH_3CHO \xrightarrow[O(a)]{4b}$$

$$CH_3COOH \xrightarrow[O(a)]{4c} (COOH)_2 \xrightarrow[O(a)]{4d}$$

$$CO_2 + H_2O$$

Reaction 4(a) is reasonable in view of the simultaneous desorption of C_2H_4O and CH_3CHO in the TPR spectra; in addition, it has been shown (*36*) that Ag is an efficient catalyst for the isomerisation $C_2H_4O \rightarrow CH_3CHO$. It is of interest to note that acetate-like intermediates have been identified in pulsed reactor studies (*37*), while oxalic acid has been proposed as an intermediate by Ide *et al.* (*38*). When C_2D_4 is oxidised, the TPR yield of oxygenated intermediates is very substantially increased. This suggests that in the sequence 4(a)–4(d) it is H-

transfer rather than C–C scission which is rate-determining for the appearance of CO_2. D for H substitution could then retard Reactions 4(a)–4(c) such that desorption of a given intermediate becomes relatively more probable.

This inhibition of the further oxidation step could also partially account for the isotopically induced change in selectivity which was observed in the batch reactor measurements. In these experiments, a kinetic isotope effect of $k_D/k_H = 0.5$ was found for CO_2 production. Again, this suggests that C–H cleavage is rate-determining, and under our conditions (relatively low selectivity) this indicates that C–H bond breaking is the crucial step in Reaction 1. That is, both the CO_2 forming Reactions 1 and 4 exhibit a normal isotope effect. The magnitude of this effect is of the right order for C–H and C–D bonds at 500 K.

A large inverse isotope effect ($k_D/k_H \sim 6.5$) was found for C_2H_4O production; qualitatively similar results have been reported with Ag sponge and Ag powder catalysts (*8*, *45*). An equally large inverse kinetic isotope effect has been reported, though not explained, in the case of propylene oxidation (*8*). Under the present scheme, it is possible to see qualitatively why there is a comparatively large isotope effect on the C_2H_4O rate because D-substitution favourably affects the branching ratio of *both* the primary and secondary steps. We will return to this question of isotope effects in what follows.

Let us now consider the primary chemistry in more detail. O_2(a) is neglected on the basis of the TPR data, and the α-CO_2 TPR peak may be associated with the direct route to total oxidation (Reaction 1); this view is reinforced by studying the effects of alkali promoters (*39*). It seems likely (*26*) that the reaction proceeds by progressive stripping of the weakly acidic hydrogens by basic O(a) species. Assuming that this involves interaction with an Ag(δ^+)-chemisorbed ethylene molecule (*30*, *40*) one may write formally

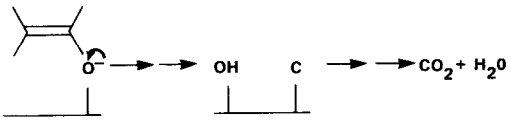

On the other hand, we propose that selective oxidation results from an electrophilic attack by O(a) on the olefinic π-bond. Again, formally:

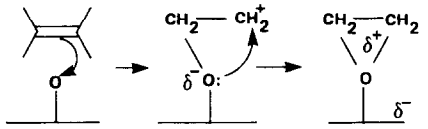

This sequence is consistent with the observation that there is almost no retention of configuration upon epoxidation of either *cis* or *trans*-1,2-d_2-ethylene (*8*, *44*, *17*). If the same type of ethylene species is involved in both Reactions 1 and 2, a simple unified mechanism can be proposed which accounts for most experimental findings. Let us assume that it is an adsorbed molcule of ethylene: this is at least consistent with our observation that oxygen chemisorption followed by *ethylene chemisorption* leads both to total oxidation (by two routes) *and* to selective oxidation. The competition between Reactions 1 and 2 is controlled by the effective charge state of O(a): total oxidation is initiated by charge transfer *from* O(a) (Reaction 1(b)); selective oxidation is initiated by charge transfer *to* O(a) (Reaction 2(a)). Thus the higher the electronic charge on O(a) the more favoured total oxidation becomes relative to selective oxidation. The effect of O(d) can now be explained: bulk oxygen competes with O(a) for metal electrons, the negative charge on O(a) is reduced and the partial oxidation channel competes effectively. The effect of Cl as a selectivity-enhancing moderator can equally well be rationalised: Cl(a) also acts to reduce the charge state of O(a), again favouring the epoxidation pathway at the

expense of CO_2 production. The decrease in selectivity which results from increased pressure (batch reactor) or increased ethylene coverage may be explained thus: (a) increased ethylene adsorption involves increased charge transfer to the metal; (b) this should increase the negative charge on O(a); (c) the selectivity should then decrease by the above arguments.

Van Santen *et al.* (*45*) have systematically investigated the effect of Cl-induced changes in selectivity on the magnitude of the isotope effect. They point out that the modified Worbs/Sachtler dioxygen mechanism requires yet another modification in order to account for the observed *reduction* in the isotope effect with *increasing* selectivity (*45*). These observations may also be understood quite simply in terms of the mechanism proposed here, and without the need for any additional assumptions. Cl moderation acts to favour Reaction 2 at the expense of Reaction 1 in the manner already explained: Reaction 2 is not subject to a deuterium kinetic isotope effect. The observed decrease in this effect with increasing Cl coverage is then understandable.

The central underlying assumption of this model is that just a single type of adsorbed ethylene and a single type of adsorbed oxygen are involved; variations in selectivity are rationalised in terms of the way in which the charge state on O(a) affects the relative rates of competing reactions. This view has the merit of simplicity and it appears to be in accord with our own observations. However, some authors have suggested that ethylene oxide formation depends on an Eley–Rideal reaction between a *gaseous* ethylene molecule and an adsorbed oxygen species. If this is correct then our simple model cannot be correct in detail. There is no doubt that we *can* make ethylene oxide under conditions which seem to point to a Langmuir–Hinshelwood mechanism, i.e., the TPR observations involving sequential dosing of oxygen and ethylene. One could try to accommodate these observations within an Eley–Rideal scheme by postulating that when O(a) is exposed to gaseous C_2H_4 the interaction proceeds immediately to the stage 2(b) even at 300 K. The resulting ethylene oxide can then be observed in a subsequent TRP sweep; under normal reaction conditions (~500 K) it would be desorbed immediately. However, one then loses the simple explanation for selectivity in terms of the branching ratio for Reactions 1 and 2. It is not easy under any scheme to suggest a clear-cut reason for the temperature dependence of the selectivity (which is of course in line with the measured activation energies). It *may* be connected with the increased mobility of O(a) at higher temperatures; this could facilitate combustion of strongly localised C and C_2 fragments.

CONCLUSIONS

1. The presence of O(a) and O(d) are necessary and sufficient conditions for the production of ethylene oxide by unsupported, unpromoted and unmoderated single crystal Ag surfaces.

2. Under TPR conditions, chemisorbed dioxygen appears to play no direct role in the surface chemistry. O(a) is responsible for *both* CO_2 *and* C_2H_4O production; absence of O(d) switches off one pathway to CO_2.

3. The two pathways to CO_2 are the direct combustion of C_2H_4 and the further oxidation of C_2H_4O. The first of these does not require the presence of O(d). The second appears to proceed via CH_3CHO, CH_3COOH, and $(COOH)_2$.

4. The kinetic isotope effects indicate that C–H scission is rate-determining in both pathways to CO_2.

5. The single crystal rate parameters are in satisfactory accord with published data for conventional catalysts.

6. It is possible to account for these observations and a number of others in terms of a simple, unified scheme which calls for the presence of just one type of adsorbed C_2H_4 and just one type of O(a). The pivotal

feature which determines selectivity is the charge state of the chemisorbed atomic oxygen.

7. It is not clear whether the proposed mechanism is applicable in all its details at higher pressures; the possibility exists that other phenomena may intervene.

ACKNOWLEDGMENTS

One of us (R.B.G.) acknowledges financial support from the SERC and I.C.I. PLC. We are grateful to Johnson Matthey Ltd. for the loan of precious metals.

REFERENCES

1. Kilty, P. A., and Sachtler, W. M. H., *Catal. Rev.-Sci. Eng.* **10,** 1 (1974).
2. Sachtler, W. M. H., Backx, C., and van Santen, R. A., *Catal. Rev.-Sci. Eng.* **23,** 127 (1981).
3. Clayton, R. W., *Chem. Soc. Spec. Period. Rep.—Catal.* **3,** 70 (1980).
4. Hucknell, D. J., "Selective Oxidation of Hydrocarbons," Chap. 2. Academic Press, New York, London, 1974.
5. Kagawa, S., Iwamoto, M., Mori, H., and Seiyama, T., *J. Phys. Chem.* **85,** 434 (1981).
6. Force, E. L., and Bell, A. T., *J. Catal.* **38,** 440 (1975).
7. Force, E. L., and Bell, A. T., *J. Catal.* **40,** 356 (1975).
8. Cant, N. W., and Hall, W. K., *J. Catal.* **52,** 81 (1978).
9. Akimoto, M., Ichikawa, K., and Echigoya, E., *J. Catal.* **76,** 333 (1982).
10. Engelhardt, H. A., and Menzel, S., *Surf. Sci.* **57,** 591 (1976).
11. Kilty, P. A., Rol, N. C., and Sachtler, W. M. M., *in* "Proceedings, 5th International Congress on Catalysis, Palm Beach, 1972." (J. W. Hightower, Ed.), p. 929. North Holland, Amsterdam, 1973.
12. Rao, C. N. R., Kamath, D. V., and Yashonath, S., *Chem. Phys. Ltt.* **88,** 13 (1982).
13. Clarkson, R. B., and Cirillo, A. C., *J. Catal.* **33,** 392 (1974).
14. Backx, C., de Groot, C. P. M., and Biloen, P., *Surf. Sci.* **104,** 300 (1981).
15. Grant, R. B., and Lambert, R. M., *J. Chem. Soc. Chem. Commun.*, 58 (1983).
16. Kobayashi, M., *in* "Catalysis under Transient Conditions" (A. T. Bell and L. L. Hegedus, Eds.), Vol. 178. Amer. Chem. Soc., Symp. Ser., Washington, D.C., 1980.
17. Egashira, M., Kuczkowski, R. L., and Cant, N. W., *J. Catal.* **65,** 297 (1980).
18. Herzog, V. M., *Ber. Bunsenges. Phys. Chem.* **74,** 216 (1970).
19. Charman, H. B., Dell, R. M., and Teale, S. S., *Trans. Faraday Soc.* **59,** 453 (1963).
20. Yokoyama, S., and Miyahara, K., *J. Res. Inst. Catal., Hokkaido Univ.* **22,** 63 (1974).
21. Backx, C., Moolhuysen, J., Geenen, P., and van Santen, R. A., *J. Catal.* **72,** 364 (1981).
22. Haul, R., Hoge, D., Neubaer, G., and Zeeck, U., *Surf. Sci.* **122,** L622 (1982).
23. Stoukides, M., and Vayenas, C. G., *J. Catal.* **70,** 137 (1981).
24. Barteau, M. A., and Madix, R. J., *Surf. Sci.* **103,** L171 (1981).
25. Rovida, G., Pratesi, F., and Ferroni, E., *Appl. Surf. Sci.* **5,** 121 (1980).
26. Wachs, I. E., and Keleman, S. R., *Surf. Sci.* **97,** L370 (1980).
27. Smith, J. N., Palmer, R. L., and Vroon, D. A., *J. Vac. Sci. Technol.* **10,** 373 (1973).
28. Kummer, J. T., *J. Phys. Chem.* **60,** 666 (1956).
29. Woodward, J. W., Lindgren, R. G., and Corcoran, W. H., *J. Catal.* **25,** 292 (1972).
30. Backx, C., de Groot, C. P. M., and Biloen, P., *Appl. Surf. Sci.* **6,** 256 (1980).
31. Felter, T. E., Weinberg, W. H., Zhdan, P. A., and Boreskov, G. K., *Surf. Sci.* **97,** L313 (1980).
32. Grant, R. B., and Lambert, R. M., *Surf. Sci.* **146,** 256 (1984).
33. Cornu, A., and Massot, R., "Compilation of Mass Spectral Data," Vol. 1, pp. 1, 2. Hayden, New York, 1979.
34. George, Z. M., and Habgood, H. W., *J. Phys. Chem.* **74,** 1502 (1970).
35. Barteau, M. A., and Madix, R. J., *Surf. Sci.* **115,** 355 (1982).
36. Grant, R. B., and Lambert, R. M., *J. Catal.*, in press.
37. Kobayashi, M., and Kobayashi, H., *J. Chem. Soc. Chem. Commun.*, 1033 (1973).
38. Ide, Y., Takagi, T., and Keii, T., *Nippon Kageku Zasshi* **86,** 1249 (1965).
39. Grant, R. B., and Lambert, R. M., *J.A.C.S. Langmuir*, in press.
40. Marcinkowsky, A. E., and Berty, J. M., *J. Catal.* **29,** 494 (1973).
41. Kanoh, H., Nishimura, T., and Ayame, A., *J. Catal.* **57,** 372 (1979).
42. Twigg, G. H., *Proc. R. Soc. London Ser. A* **188,** 92 (1946).
43. Kenson, R. E., and Lapkin, M., *J. Phys. Chem.* **74,** 1493 (1970).
44. Larrabee, A. L., and Kuczkowski, R. L., *J. Catal.* **52,** 72 (1978).
45. van Santen, R. A., Moolhuysen, J., and Sachtler, W. M. H., *J. Catal.* **65,** 478 (1980).